Conical and Bi-conical High-Q Optical-Nanofiber Microcoil Resonator

Fei Xu, Peter Horak, and Gilberto Brambilla
Optoelectronics Research Centre, University of Southampton,
Southampton SO17 1BJ, United Kingdom

ABSTRACT

The Q-factor of the optical nanowire microcoil resonator is calculated and compared for different geometries. The results suggest that the Q-factor is very sensitive to the coupling conditions and high-Q resonators can be obtained more easily when the geometry of the nanowire microcoil resonator or its coupling contour has a bi-conical profile.

Keywords: Microfibers, optical nanowire, optical fiber coupling, optical resonators, ring resonators

1. INTRODUCTION

High-Q microresonators have found numerous applications, for example in microlasers, narrow filters, optical switching, ultrafine sensing, displacement measurements, high resolution spectroscopy, and studies of nonlinear optical effects. The investigated structures include whispering gallery resonators [1-4], microring resonators [5-7], micropost (or micropillar) cavities [8], photonic crystal defect microcavities [9] and more recently the self-coupling nanowire coil resonator [10-15]. The optical nanowire microcoil resonator (ONMR) is a three-dimensional generalization of the loop/ring resonator. It can be realized by wrapping an optical nanowire on a low index dielectric rod [12-15]. Since it is fabricated from a single mode fiber, the ONMR has a unique advantage in coupling light in and out of the resonator. With recent progress in the fabrication of low-loss optical nanowires [16-19], the Q-factor of ONMRs could potentially compete with the highest Q-factors currently available in microresonators, i.e., with the Q-factors of whispering gallery modes in silica microspheres or microdisks [20]. In this paper we investigate the dependence of the Q-factor of ONMRs on coupling parameters in different geometries and demonstrate that the uniform profile is not the optimal profile to easily obtain high Q-factors.

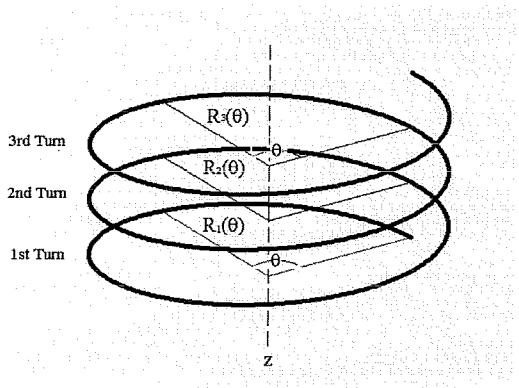

Fig. 1. Illustration of an ONMR in cylindrical coordinates.

2. THEORETICAL MODEL

The results described in the later sections of this work are obtained from numerical solutions of a set of coupled wave equations as outlined in the following. In the ONMR illustrated in Fig. 1, $A(\theta)$ is defined as the light field amplitude at position $(\theta, R(\theta))$ in a cylindrical coordinate system, where $R(\theta)$ is the distance from the z-axis and θ is the angle coordinate. It is convenient to define the amplitude $A_m(\theta)$ of the field at the m^{th} turn and to consider θ as the common

coordinate along turns, so that $0 < \theta < 2\pi$. The propagation of light along the coil in an M-turn ONMR is then described by the coupled wave equations [10]:

$$\frac{d}{d\theta}\begin{pmatrix} A_1 \\ A_2 \\ \cdots \\ A_m \\ \cdots \\ A_{M-1} \\ A_M \end{pmatrix} = i\begin{pmatrix} 0 & R_1(\theta)\chi_{12}(\theta) & 0 & \cdots & 0 & 0 & 0 \\ R_2(\theta)\chi_{21}(\theta) & 0 & R_2(\theta)\chi_{23}(\theta) & \cdots & 0 & 0 & 0 \\ 0 & R_3(\theta)\chi_{32}(\theta) & 0 & \cdots & 0 & 0 & 0 \\ \cdots & \cdots & \cdots & \cdots & \cdots & \cdots & \cdots \\ 0 & 0 & 0 & \cdots & 0 & R_{M-2}(\theta)\chi_{M-1M-2}(\theta) & 0 \\ 0 & 0 & 0 & \cdots & R_{M-1}(\theta)\chi_{M-2M-1}(\theta) & 0 & R_{M-1}(\theta)\chi_{M-1M}(\theta) \\ 0 & 0 & 0 & \cdots & 0 & R_M(\theta)\chi_{MM-1}(\theta) & 0 \end{pmatrix}\begin{pmatrix} A_1 \\ A_2 \\ \cdots \\ A_m \\ \cdots \\ A_{M-1} \\ A_M \end{pmatrix} \quad (1)$$

where

$$\chi_{pq}(\theta) = \kappa_{pq}(\theta)\exp\left\{i\int_0^{2\pi}\beta_p(\theta)R_p(\theta)d\theta - i\int_0^{2\pi}\beta_q(\theta)R_q(\theta)d\theta\right\}, \quad (2)$$

β is the propagation constant, and κ_{pq} is the coupling coefficient between the p^{th} and q^{th} turns [9]. Here only the coupling between two adjacent turns is considered, and the coefficient β is supposed to be independent of θ. At $\theta = 2\pi$, the coils and the field amplitudes must be continuous, which leads to the continuity conditions:

$$R_{m+1}(0) = R_m(2\pi), \quad (3)$$

$$A_{m+1}(0) = A_m(2\pi)\exp\left\{i\int_0^{2\pi}\beta R_m(\theta)ds\right\}, m = 1,2,\ldots M-1. \quad (4)$$

We introduce the average radius R_0, the coupling parameter K_{pq}, the transmission amplitude T, and the Q-factor Q defined as

$$R_0 = \left(\sum_{m=1}^{M}\int_0^{2\pi}R_m(\theta)d\theta\right)\Big/2\pi M, \quad (5)$$

$$K_{pq} = 2\pi R_0\kappa_{pq}(\theta), \quad (6)$$

$$T = \frac{A_M(2\pi)}{A_1(0)}\exp\left\{i\int_0^{2\pi}\beta R_M(\theta)d\theta\right\}, \quad (7)$$

$$Q = \frac{\lambda_0}{\Delta\lambda}, \quad (8)$$

where $\Delta\lambda$ is the full width at half maximum (FWHM) of the transmission spectrum or the group delay near the wavelength λ_0 [21]. If propagation losses are ignored, β is real and $|T|=1$. In this case, the coil performs as an all-pass filter and the resonances of the transmission coefficient appear in the group delay only. Furthermore, in the lossless case the FWHM of the resonances approaches zero and thus the Q-factor becomes infinite. For the realistic case of a nanowire with finite loss, the FWHM has a non-zero minimum. The actual value of the FWHM depends on the ONMR geometry, which is characterized by the diameter $R_m(\theta)$ of the individual turns, and on the spatial variation of the coupling constant $\chi_{pq}(\theta)$, which is determined by the microcoil pitch.

For the results presented here, we numerically solved Eq. (1) assuming a nanowire diameter of D=1000 nm, a fiber refractive index of 1.46 with an effective index of n_{eff}=1.2 at a wavelength of 1.55 μm, R_0=125/2 μm, and a propagation loss of ~0.02 dB/mm. The coupling parameter K is very sensitive to the distance between the central axes of adjacent

turns: it is maximum ($K_M \sim 20$) when two turns touch (the distance between them is equal to their diameter D), and $K \sim 4$ when the distance is increased to $1.5D$. For our simulations, we scan K through the entire range from 0 to K_M.

Fig. 2 shows the transmission spectra of two ONMRs with M=3 and 4 turns, respectively, with constant diameter $R_m(\theta)=R_0$ and constant coupling $K=2\pi$. Both spectra are periodic, with one sharp transmission peak per period for M=3, and two peaks per period for M=4. In the following we investigate the parameter dependence of the FWHM of the peak closest to the central wavelength (1550 nm); for the spectra shown in Fig. 2, for example, these are peak A for M=3 and peak B for M=4.

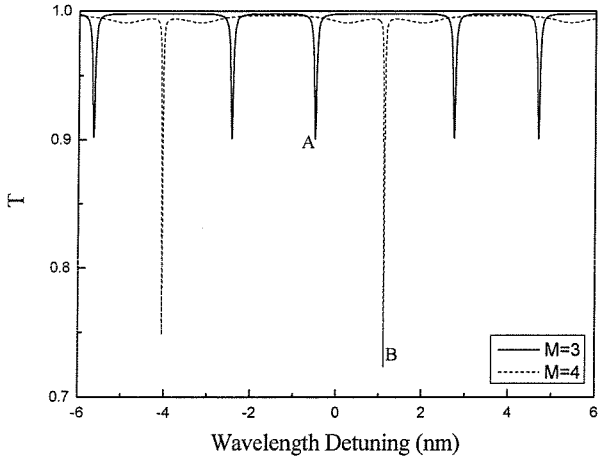

Fig. 2. Transmission spectra of three-turn and four-turn ONMRs at wavelengths near 1550 nm.

3. FWHM AND Q-FACTOR IN DIFFERENT GEOMETRIES

In this section, we investigate the effect of different geometries on the FWHM and on the Q-factor of ONMRs. To this end we suppose that the coupling coefficient κ is independent of θ, i.e., that the pitch between adjacent turns of the coil is constant and thus the coupling parameter K is constant. The radii of the individual turns, on the other hand, are assumed to vary with angle θ and turn index m.

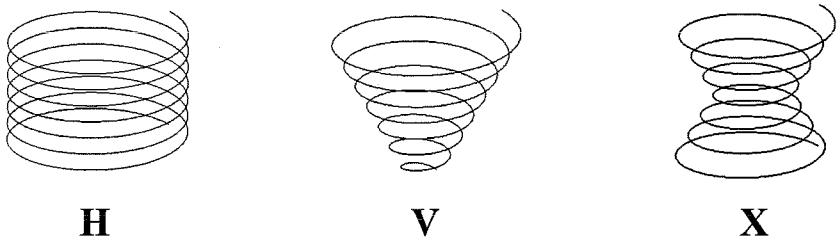

Fig. 3. Illustration of ONMRs with three geometries: H (cylindrical), V (conical), and X (biconical) profiles.

We consider the three simple fundamental geometries illustrated in Fig. 3, given by the following profiles:

H (Cylindrical): $R_m(\theta) = R_0$, (9a)

V (Conical): $R_m(\theta) = R_0 + \frac{M}{2} dR + (m - 1 + \frac{\theta}{2\pi}) dR$, (9b)

$$\text{X (Biconical):} \quad R_m(\theta) = R_0 + \left|\left(\frac{M+1}{2} - m - \frac{\theta-\pi}{2\pi}\right)\right| dR - \frac{M}{4} dR, \tag{9c}$$

where m=1,2…M, dR/R_0<<1, and $|R_{m+1}(\theta)-R_m(\theta)|=dR$ for all m. Here we use dR=0.1 μm.

The FWHM of the transmission peak near 1550 nm for the three profiles has been calculated from Eqs. (1)-(8). The resulting dependence of the FWHM on K is shown in Fig. 4 for M=3 and 4. The FWHM decreases monotonically with K when K is very small (K<1), but fluctuates widely for larger values of K. Thus, in general high Q-factors cannot be obtained simply by increasing K, i.e. by bringing adjacent turns closer together. For M=3 the FWHM of the H profile is nearly periodic in K and close to the minimum at $K=K_M$. For M=4, on the other hand, the FWHM fluctuates in an irregular way and is relatively large at $K=K_M$. More specifically, at $K=K_M$ our simulations predict $\Delta\lambda$=0.02 nm for M=3 and 0.25 nm for M=4, respectively. The minimum of the FWHM is ~0.002 nm for all profiles because of the finite propagation loss in the nanowire.

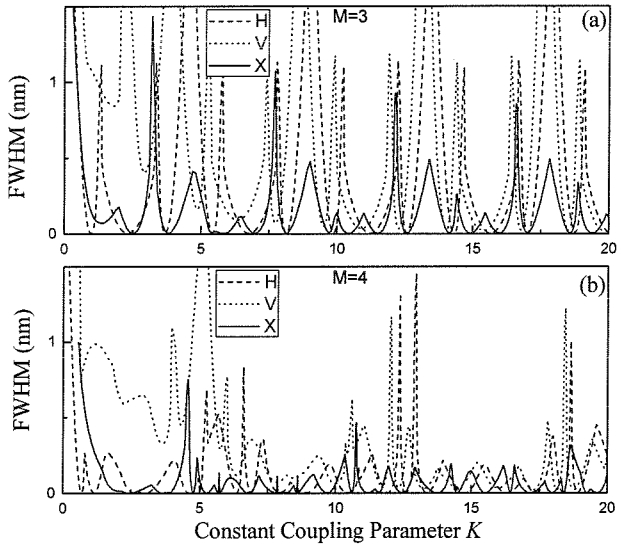

Fig. 4. The FWHM dependence on the constant coupling parameter K near λ_0=1550 nm for three geometries: H (dashed lines), V (dotted lines) and X (solid lines) profiles. (a) M=3, (b) M=4.

For most applications it is desirable to maximize the Q-factor of the ONMR. In principle, this can be achieved by selecting a K for which the FWHM is minimized. However, fabrication of the corresponding ONMR is extremely difficult because K is enormously sensitive to the distance between adjacent turns. It is therefore preferable to find ONMR geometries and/or coupling profiles for which the FWHM varies slowly with K. As shown in Fig. 4, we find that an X-shaped resonator has a flatter FWHM than one with profile H, and profile H has a flatter FWHM than profile V. This implies that some geometries may lead to easier fabrication of high-Q resonators than others. In order to quantify this effect, we introduce the "tolerance ratio" which we define as the fraction of K values where the FWHM is close to the minimum within a given interval. In practical terms, the tolerance ratio is the probability that an arbitrarily chosen value of K will result in an ONMR with near-maximum Q-factor. Specifically, we consider FWHM<0.01 nm in the whole interval K=0 to K_M and in the smaller interval K=0.8K_M to K_M.

Fig. 5 shows the tolerance ratios for ONMRs with M=3-9 turns, which are considered a feasible target with the current technology. The tolerance ratios of the H and X profiles increase quickly with M. This indicates that high Q-factors are readily achieved by fabricating resonators with as many turns as possible. Note however that this assumes a high degree

of accuracy over the entire structure, which is extremely challenging to maintain under practical fabrication conditions. The X profile is the optimal shape and its tolerance ratio is nearly 50% larger than that of the H profile. The V profile is by far the worst geometry, with a tolerance ratio close to zero. Therefore, the X profile provides the largest choice of K values to achieve an optimal Q-factor.

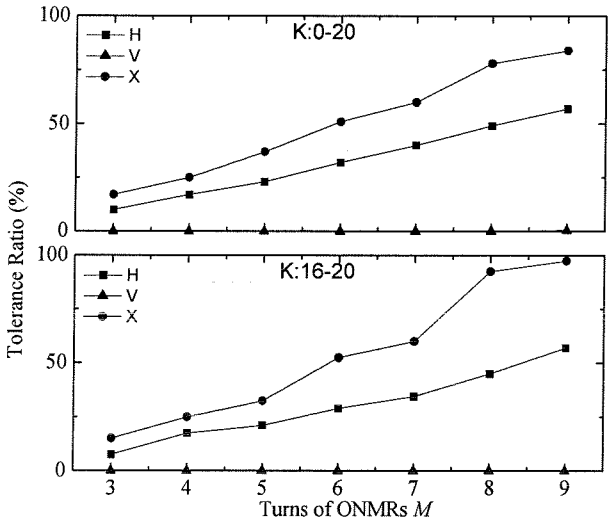

Fig. 5. Dependence of the tolerance ratio (defined as the fraction of values of the average coupling parameter K where the FWHM is below 0.01 nm) in the whole range (0-20) and in a smaller range near K_M (16-20) on the number of turns M in a microcoil resonator for three geometries: H (squares), V (triangles) and X (circles) profiles.

4. FWHM AND Q-FACTOR IN DIFFERENT COUPLING PROFILES

In Section 3, the coupling parameter was supposed constant and only the resonator geometry was changed. By contrast, in this section we will investigate the effects of varying the coupling parameter along the length of the microcoil while keeping the coil radius constant. We expect that fabrication of such ONMRs will be even more challenging than the fabrication of ONMRs of varying geometry as described above, since varying the coupling profile requires a controlled and extremely accurate design of the pitch along the length of the ONMR.

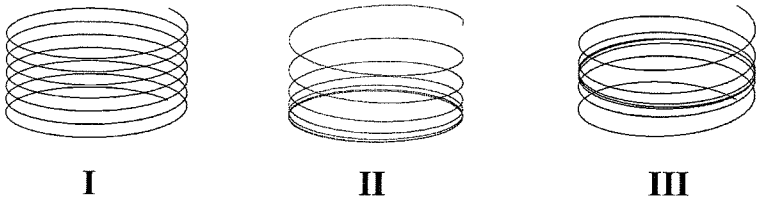

Fig. 6. Illustration of the three different coupling profiles.

The three different coupling profiles illustrated in Fig. 6 will be discussed in the following. Profile I is the uniform case with constant coupling already discussed in Section 3; profile II exhibits an increasing pitch from the bottom to the top;

and profile III has an increasing pitch from the center to the edges. Defining the coupling parameter $K_{pp+1}(\theta)=2\pi R_0\kappa_{pp+1}(\theta)$, the three profiles can be expressed as:

$$\text{I (Uniform):} \qquad K_{pp+1}(\theta) = K_c, \tag{10a}$$

$$\text{II (Linear):} \qquad K_{pp+1}(\theta) = K_c(p-1+\theta/2\pi)/(M-1), \tag{10b}$$

$$\text{III (Triangle):} \qquad K_{pp+1}(\theta) = K_c\left(1-\left|\frac{(p-1+\theta/2\pi)}{(M-1)/2}-1\right|\right), \tag{10c}$$

where $p=1,2...M-1$ and K_c is the maximum coupling parameter.

As previously, we calculate the FWHM of the transmission peak closest to 1550 nm wavelength by solving Eqs. (1)-(8). Fig. 7 shows the dependence of the FWHM on K for the three profiles when M=3 and 4. The most important observation here is that profile III exhibits a very small and flat FWHM for all values of K>10 for M=3 and for K>4 for M=4.

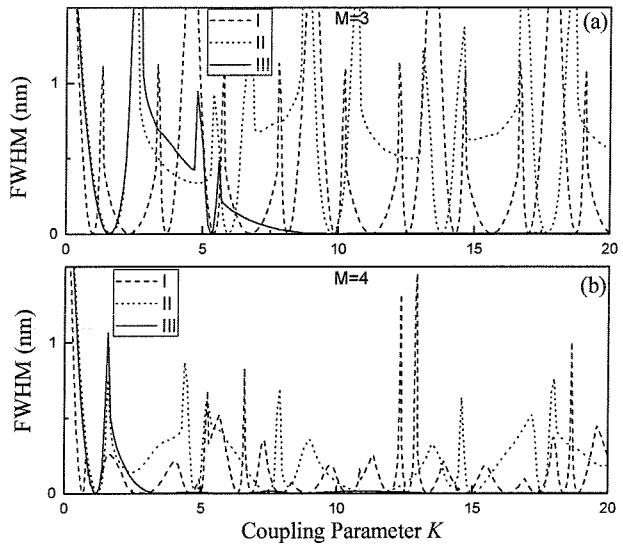

Fig. 7. FWHM of the transmission peak near λ_0=1550 nm versus coupling parameter K_c for coupling profiles I (dashed lines), II (dotted lines), and III (solid lines) for (a) M=3 and (b) M=4.

The tolerance ratios of the three coupling profiles for M=3-9 are shown in Fig. 8. Coupling profiles II and III present a similar behavior to the geometric profiles V and X discussed in Sec. 3. The tolerance ratio is always very large (near 100%) for profile III and very small (<15%) for profile II. Note that limiting the sampling range of K can modify the behavior of the tolerance ratio as observed in Fig. 8 for profile III and K=16 to 20, where the tolerance ratio is no longer increasing monotonically with M but has a marked minimum at M=5. The reason for this effect can be seen more clearly on a logarithmic plot of the FWHM versus the coupling parameter, shown in Fig. 9. The FWHM fluctuates widely, and thus the tolerance ratios increase monotonically only when the sampling range of K is sufficiently large (for example 0-20).

These results show clearly that high-Q-factor ONMRs can be achieved more easily by a gradual increase of the microcoil pitch from the center towards the two ends. However, the actual fabrication of ONMRs with variable coupling profiles remains a very challenging task with current technology.

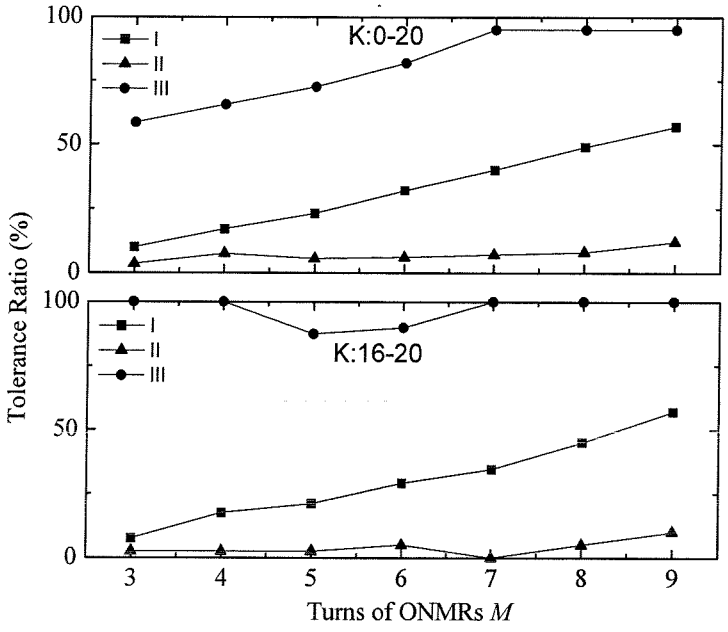

Fig. 8. Dependence of the tolerance ratio on the number of turns M in a microcoil resonator for coupling profiles I (squares), II (circles), and III (triangles), for a wide range of K (0-20, top) and for a small range near K_M (16-20, bottom)

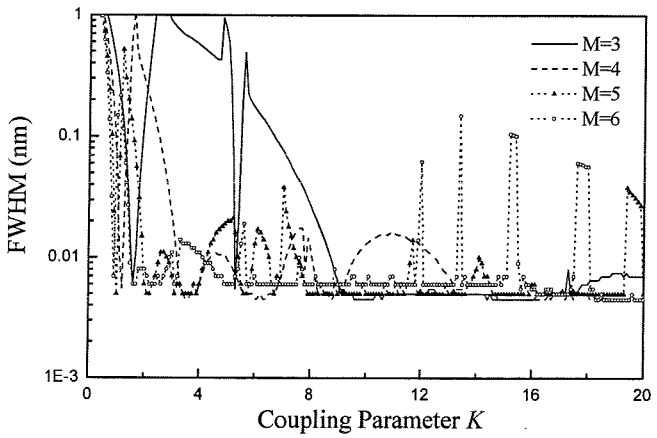

Fig. 9. FWHM near λ_0=1550 nm versus coupling parameter K_c on a logarithmic scale for the coupling profile III.

5. SUMMARY AND CONCLUSION

The coupled wave equations for optical-nanofiber microcoil resonators have been solved for different geometries and different coupling profiles. Two routes towards improved tolerance of the Q-factor on the value of the coupling parameter between adjacent turns have been identified. (i) Wrapping the microcoil with constant pitch around a low-refractive-index rod with a bi-conical profile results in increased tolerance, in particular for ONMRs with a few (<10) turns. (ii) A microcoil wrapped around a cylindrical rod with a pitch increasing from the center towards the ends gives high tolerance even for coils of only 3 turns. Both schemes are technologically very challenging, but promise significant improvements over the generic design of a coil of constant pitch on a cylindrical rod.

ACKNOWLEDGMENT

The authors gratefully acknowledge discussions with Dr. Wei Loh and Prof. David J. Richardson who initiated this research. This work was supported by the EPSRC under the standard research grant EP/C00504X/1.

REFERENCES

1. V. B. Braginsky, M. L. Gorodetsky, and V. S. Ilchenko, "Quality-factor and nonlinear properties of optical whispering-gallery modes," *Phys. Lett. A*, 137, 393-397, 1989.
2. J. C. Knight, G. Cheung, F. Jacques, and T. A. Birks, "Phase-matched excitation of whispering-gallery mode resonances by a fiber taper," *Opt. Lett.*, 22, 1129-1131, 1997.
3. V. I. Ilchenko, A. A. Savchenkov, A. B. Matsko, and L. Maleki, "Dispersion compensation in whisperinggallery modes," *J. Opt. Soc. Am. A*, 20, 157, 2003.
4. S. M. Spillane, T. J. Kippenberg, O. J. Painter, and K. J. Vahala, "Ideality in a Fiber-Taper-Coupled Microresonator System for Application to Cavity Quantum Electrodynamics," *Phys. Rev. Lett.*, 91, 04902, 2003.
5. B. E. Little, S. T. Chu, H. A. Haus, J. Foresi, and J. P. Laine, "Microring resonator channel dropping filters," *J. Lightwave Technol.*, 15, 998-1005, 1997.
6. D. Rafizadeh, J. P. Zhang, S. C. Hagness, A. Taflove, K. A. Stair, and S. T. Ho, "Waveguide-coupled AlGaAs/GaAs microcavity ring and disk resonators with high finesse and 21.6-nm free spectral range," *Opt. Lett.*, 22, 1244-1246, 1997.
7. S. T. Chu, B. E. Little, W. Pan, T. Kaneko, S. Sato, and Y. Kokubun, "An eight-channel add-drop filter using vertically coupled microring resonators over a cross grid," *IEEE Photon. Technol. Lett.*, 11, 691-693, 1999.
8. J. M. Gerard, D. Barrier, J. Y. Marzin, R. Kuszelewicz, L. Manin, E. Costard, V. Thierry-Mieg, and T. Rivera, "Quantum boxes as active probes for photonic microstructures: The pillar microcavity case," *Appl. Phys. Lett.*, 69, 449-451, 1996.
9. O. Painter, R. K. Lee, A. Scherer, A. Yariv, J. D. O'Brien, P. D. Dapkus, and I. Kim, "Two-dimensional photonic band-gap defect mode laser," *Science*, 284, 1819-1821, 1999.
10. M. Sumetsky, Y. Dulashko, J. M. Fini, A. Hale, and D. J. DiGiovanni, "The Microfiber Loop Resonator: Theory, Experiment, and Application," *J. Lightwave Technol.* 24, 242-249, 2006
11. M. Sumetsky, Y. Dulashko, and A. Hale, "Fabrication and study of bent and coiled free silica nanowires: Self-coupling microloop optical interferometer," *Opt. Express* 12, 3521-3531, 2004
12. M. Sumetsky, "Optical fiber microcoil resonator," *Opt. Express*, 12, 2303-2316, 2004.
13. M. Sumetsky, "Uniform coil optical resonator and waveguide: transmission spectrum, eigenmodes, and dispersion relation," *Opt. Express*, 13, 4331-4340, 2005.
14. M. Sumetsky, "Fiber coil optical microresonators," in Biophotonics/Optical Interconnects and VLSI Photonics/WBM Microcavities, 2004 Digest of the LEOS Summer Topical Meetings 28-30, 2004
15. M. Sumetsky, "Microcoil photonic resonator and waveguide," in *Optical Fiber Communication Conference*, 2005. Technical Digest. OFC/NFOEC, 5, 6-11, 2005
16. L. M. Tong, R. R. Gattass, J. B. Ashcom, S. L. He, J. Y. Lou, M. Y. Shen, I. Maxwell, and E. Mazur, "Subwavelength-diameter silica wires for low-loss optical wave guiding," *Nature,* 426, 816-819, 2003.
17. G. Brambilla, V. Finazzi, and D. J. Richardson, "Ultra-low-loss optical fiber nanotapers," *Opt. Express*, 12, 2258-2263 (2004),
18. G. Brambilla, F. Xu, X. Feng, "Fabrication of optical fibre nanowires and their optical and mechanical characterization," *Electron. Lett.*, 42, 517-519, 2006.

19. A. M. Clohessy, N. Healy, D.F. Murphy and C.D. Hussey, "Short low-loss nanowire tapers on singlemode fibres," *Electron. Lett.,* 41, 954-955, 2005
20. K. J. Vahala, "Optical microcavities," *Nature*, 424, 839-846, 2003.
21. O. Schwelb, "Transmission, group delay, and dispersion in single-ring optical resonators and add/drop filters—A tutorial overview," *J. Lightwave Technol.,* 22, 1380-1394, 2004.